HIGH-CURRENT ^{14}C MEASUREMENTS ON AN HVE 1MV AMS SYSTEM

Matthias Klein • A Gottdang • D J W Mous

High Voltage Engineering Europa B.V., PO Box 99, 3800 AB Amersfoort, the Netherlands. Email: info@highvolteng.com.

ABSTRACT. High radiocarbon sample throughput is an increasingly important requirement of accelerator mass spectrometry (AMS) systems, which in turn requires high source output. To accomplish this, HVE AMS systems use a model SO-110B ion source, which can run at outputs of more than 200 μA ^{12}C. It is known that high source output may compromise precision. To quantify this effect, we have tested an HVE 1MV AMS system for the influence of medium (100 μA) and high (200 μA) source outputs on the precision. These early measurements indicate for a 200 μA ^{12}C source output, equivalent to a ~1 kHz ^{14}C count rate for Ox II samples, a $^{13}C/^{12}C$ precision of 1‰ and a $^{14}C/^{12}C$ precision of 3‰ can be obtained.

INTRODUCTION

Commercial radiocarbon applications have become increasingly important for many accelerator mass spectrometry (AMS) laboratories. Meeting the rising demand on sample throughput requires sufficient capacity for sample preparation, as well as fast measurements and minimal system downtime. For high measurement efficiency, the AMS system must support high source output without degradation of the measurement precision or the disproportional increase of maintenance effort.

High-current ^{14}C measurements have been done on different AMS systems, sometimes injecting no ^{12}C into the accelerator (Fallon et al. 2007; Freeman et al. 2010; Roberts et al. 2010). This article describes how increasing the source output up to ~200 μA analyzed and injected ^{12}C influences the performance of the High Voltage Engineering (HVE) 1MV AMS system with respect to precision, background, and beam transport capability.

SYSTEM DESCRIPTION

Measurements were performed on a 1MV multi-element HVE AMS model 4110Bo-AMS. It is essentially identical to the compact 1MV AMS system described elsewhere (Klein et al. 2006, 2007; see Figure 1), but equipped with a rotatable electrostatic analyzer (ESA) in the injector, which serves as a switch for the connection of a second ion source. This system uses the HVE model SO-110B cesium sputter ion source. The standard sample storage capacity of the carousel in the target chamber is 50 and can be extended to 200 for high throughput.

The source has a well-defined sputter spot of 0.5 to 1 mm diameter, depending on the cesium flow, with minimal cesium intensity in the surrounding halo having a diameter <5 mm for the highest applied cesium flow. Gaseous material is quickly removed by the turbopump on the source housing, minimizing contamination and source memory when operating at high outputs. The short- and long-term precision of the measurements is supported by the high bouncing frequency of 100 Hz and the stabilization system for the terminal voltage based on a slit system that is incorporated in the ^{13}C offset Faraday cup (Klein et al. 2004).

The AMS system has a very open ion optical transport system. Vertical beam scans showed that the magnet gaps of the analyzer magnets of 50 mm impose no limitation on beams below 200 μA ^{12}C current. The dominant constraint to beam transport is formed by the 6-mm-diameter stripper canal at the accelerator terminal.

Proceedings of the 21st International Radiocarbon Conference edited by A J T Jull & C Hatté
RADIOCARBON, Vol 55, Nr 2–3, 2013, p 224–230

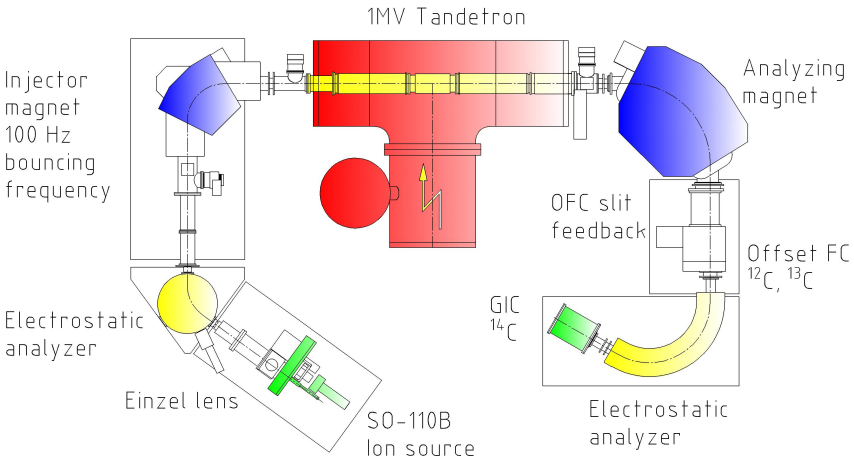

Figure 1 Layout of the HVE 1MV AMS system. The accelerator voltage is stabilized using feedback from a slit system within the ^{13}C offset Faraday cup.

RESULTS

Source Performance

For the performance tests, we used aluminum targets with a 1.3-mm central bore, into which graphitized oxalic acid sample material was pressed from the back side. When running the source for carbon outputs, the target (or cathode) voltage is 8.5 kV, supporting smooth and glitch-free operation. The source output was essentially determined by the temperature of the cesium. For its regulation, we use a sensor mounted on the cesium reservoir housing showing a temperature somewhere between that of the cesium and the heater. Medium currents around 100 µA analyzed ^{12}C require a temperature setting of about 115 °C. An increase to 130 °C results in currents of ~200 µA.

At 130 °C and upon first insertion of a sample into the source, the output currents start off at ~50 µA, reach 150 µA after ~2 min, and level off at ~200 µA. For the following insertions, these samples are presputtered and covered with cesium and the output current reaches the final value almost instantaneously.

To quantify how the beam quality decreases when the output current increases, the beam emittance was measured for various ^{12}C currents. We used an electrostatic einzel lens following the ion source (see Figure 1) to create a beam waist at the position of a beam profile monitor (BPM). From the profiles, we measured the full width at half maximum (FWHM) and tenth maximum (FWTM) beam size, corresponding to ~65% and ~95% of the total beam current. A second BPM installed ~50 cm downstream measured the divergence of the beam. The beam emittance ε (defined as the phase space area divided by π) was calculated from these measurements. The ion energy is 35 keV, the typical setting for HVE AMS injectors. The emittance values at output currents between 50 and 300 µA ^{12}C are shown in Figure 2. Typical values range from 2 to 8 mm mrad $MeV^{½}$ for FWHM and FWTM. Figure 2 shows that there is only a small increase in emittance for currents up to 200 µA. This source feature supports constant system performance for medium and high ion source output. For currents above 200 µA, the source emittance measurements indicate an increase of the beam divergence.

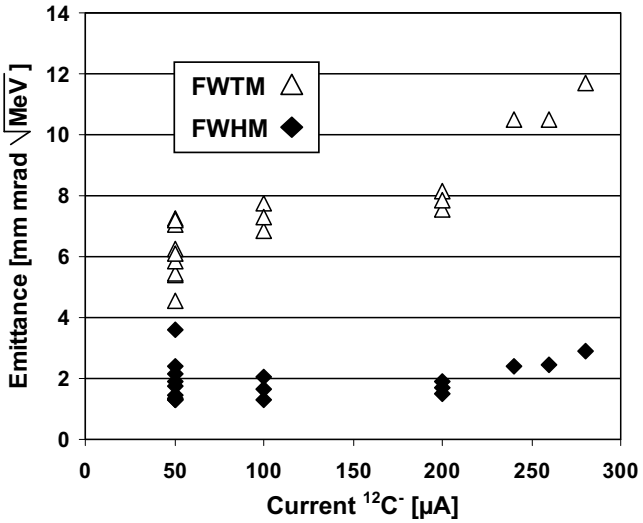

Figure 2 Emittance of the SO-110B ion source for FWHM (diamonds) and FWTM (triangles) of the beam in relation to the source output current of $^{12}C^-$.

Beam Transmission

To investigate the impact of the small stripper canal on the achievable precision, we scanned the beam across the canal while bouncing was active, using the injector magnet. The injection duty for the stable isotopes is 1%, which makes injection of the strong ^{12}C beams possible. Differences in transmission of the isotopes will create variations in the isotopic ratios. Figure 3 shows the normalized ratio $^{13}C/^{12}C$ versus the displacement in the stripper canal. At low currents, beam size and divergence are small, which results in a large "flat top" of ~3 mm for the resulting isotopic ratio, which shows the range for beam movements that do not affect the measurement result. At higher currents, this range gets smaller, but a flat top still remains. This is in line with our observation that a measured beam transmission of 45% into charge state 2+ is independent of the source output current.

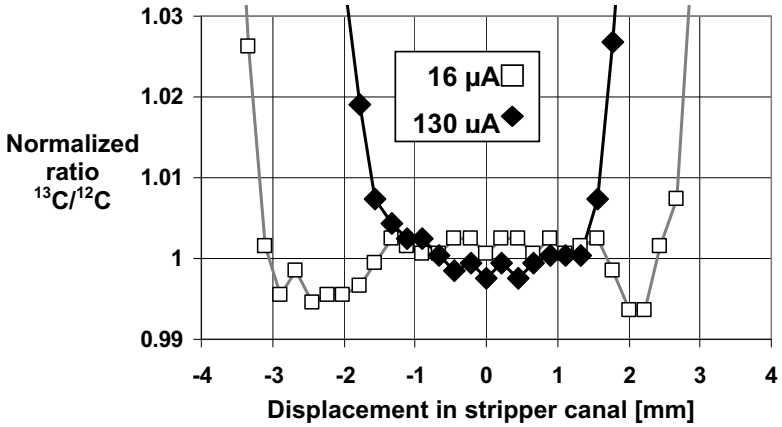

Figure 3 $^{13}C/^{12}C$ ratio versus beam displacement in the stripper canal. For low currents, the beam is small compared to the canal diameter and can be displaced by approximately ±2.5 mm without changing the isotopic ratio. For high currents, the range for displacement without ratio changes is smaller, but a clear flat top is still present.

Radiocarbon Precision Measurements

We investigated the performance of the AMS system at 2 different source output current levels: ~100 µA (medium current) and ~200 µA (high current) ^{12}C. As the particle transmission is close to 50%, these currents are measured for $^{12}C^{-}$ as well as for $^{12}C^{2+}$. These measurements were done using an identical set of system parameters, with the exception of the cesium reservoir temperature that was adjusted to regulate the source output. The system settings that were used were optimized for high currents.

Medium Current

With the source set at 115 °C for medium output, we measured three 1.3-mm-diameter oxalic acid samples labeled A, B, and C in a cyclic sequence. To compare the results for different insertions of the same sample, each analysis was stopped when 10k ^{14}C counts were acquired and then the following sample was inserted. In this way, each sample was run less than 5 min in total, during which ~80k ^{14}C counts were collected. Figure 4a shows the output current as function of the time the sample was present in the source. After an initial rise, the output stabilizes at the current level that is expected from the cesium reservoir temperature setting. Figure 4b shows the relation of the $^{13}C/^{12}C$ ratio to the $^{12}C^{2+}$ current, indicating a linear dependency. In order to eliminate this dependency, we applied a current correction for the isotopic ratio. For this correction, we did a linear fit of the data, resulting in a line with an offset ratio of 1.029% and a slope of 0.00023% per µA increase in $^{12}C^{2+}$ current. The corrected ratios were calculated as:

$$\text{corrected } {}^{13}C/{}^{12}C = (\text{mean } {}^{13}C/{}^{12}C \,/\, \text{measured } {}^{12}C^{2+} \times \text{slope} + \text{offset}) \times \text{measured } {}^{13}C/{}^{12}C$$

The averages of the corrected ratios for every sample coincided within 1.1‰.

For the ^{14}C ratios, the Poisson error of 1% for the individual analyses obscures any current dependency of the results. In these measurements, the averages for the samples scattered within 0.4‰ for $^{14}C/^{12}C$ (uncorrected: 1.3957, 1.3951, 1.3946 × 10^{-12}) and within 2.3‰ for $^{14}C/^{13}C$ (uncorrected: 1.3327, 1.3288, 1.3266 × 10^{-10}), which shows no significant difference to the error of 3.5‰ that can be expected from the Poisson statistics.

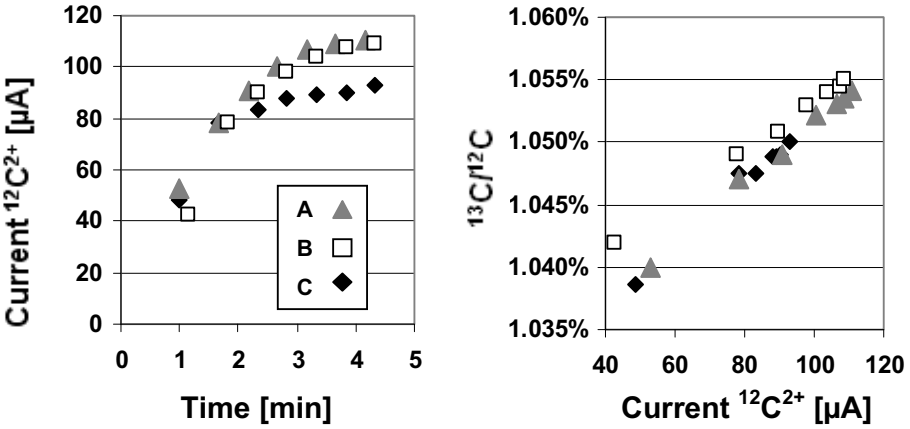

Figure 4 a) Current output versus time in the ion source for samples A, B, and C (left). b) Measured $^{13}C/^{12}C$ ratio for the same samples versus the output current (right). After a linear correction for the trend, the stable isotope ratio means of the samples agree within 1‰. The system was tuned for higher currents (see text).

Processed graphite was measured with $^{14}C/^{12}C$ ratios below 3×10^{-15}, which is typical for this kind of sample. No impact of the increased current on the background level was observed.

High Current

After the tests using medium current, we set the source to 130 °C cesium reservoir temperature for the expected high source-current output. The measurements were done on the same samples A, B, and C that had been used during the medium current tests, plus an additional sample (sample D) that was not sputtered. Figure 5a shows the $^{12}C^{2+}$ current as function of the time for these samples. For the new sample D, we see an increase in $^{12}C^{2+}$ current that exceeds 150 µA within 2 min. Sample B became depleted during the test, which is clearly visible from the drop in output current after 2 min of sputtering. Figure 5b shows the relation of the measured ratio $^{13}C/^{12}C$ to the $^{12}C^{2+}$ current. For the fresh sample D, we see in the output range below 100 µA a rising $^{13}C/^{12}C$ ratio for increasing $^{12}C^{2+}$ current, as was found for the other samples in the medium current measurements.

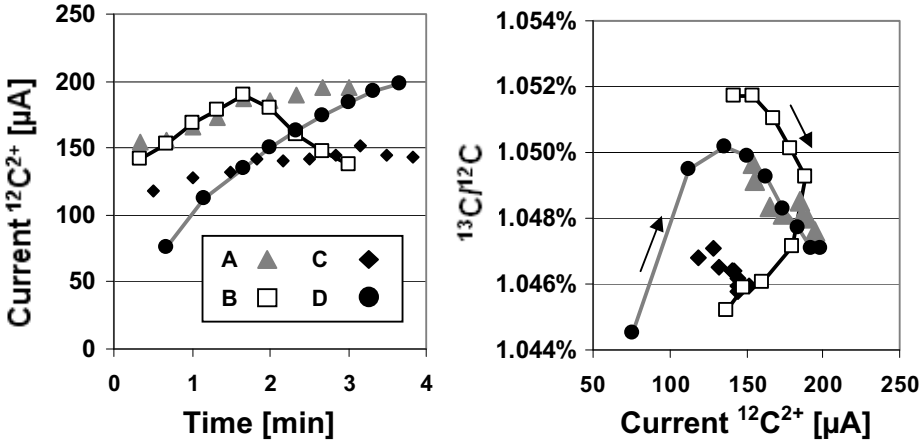

Figure 5 a) Output current versus measurement time for samples A–D at high current (left). Samples A–C have also been used for the medium current experiment. Accentuated are sample B (depleting) and D (newly introduced). b) $^{13}C/^{12}C$ ratio versus output current (right). For current variations of ~100 µA, the $^{13}C/^{12}C$ ratio varies ~5‰. The arrows indicate progress in time.

In the range between 100 and 200 µA, the ratio drops with increasing output, at least as long as the samples are not depleted. For sample B, we observed falling output after 2 min of sputtering, which indicates depletion of the sample. Sample B shows dropping ratios also for decreasing output. This kind of fractionation is seen in virtually all AMS facilities when samples are near exhaustion. The high current measurement thus includes data from samples in very different states—fast output rise at first sputtering, stable output and decreasing output at depletion—which makes it impossible to apply a simple current correction as in the previous case of medium current output. Without any corrections applied, the $^{13}C/^{12}C$ means for the different samples agree within 1‰. The $^{14}C/^{12}C$ averages for samples A to D (1.3775, 1.3730, 1.3718, and 1.3809×10^{-12}) agree within 3.1‰, in agreement with Poisson statistics.

While the previously used samples were exhausted, the new sample D produced stable output currents above 200 µA for several more minutes (see Figure 6a). During this time, the ^{14}C detector count rate increased to 0.95 kHz. This count rate is corrected for effects of the detector dead time,

which exceeds 1% at these high currents. When the output was stable and the sample not depleted, not much change in the $^{13}C/^{12}C$ ratio was noticed (Figure 6b).

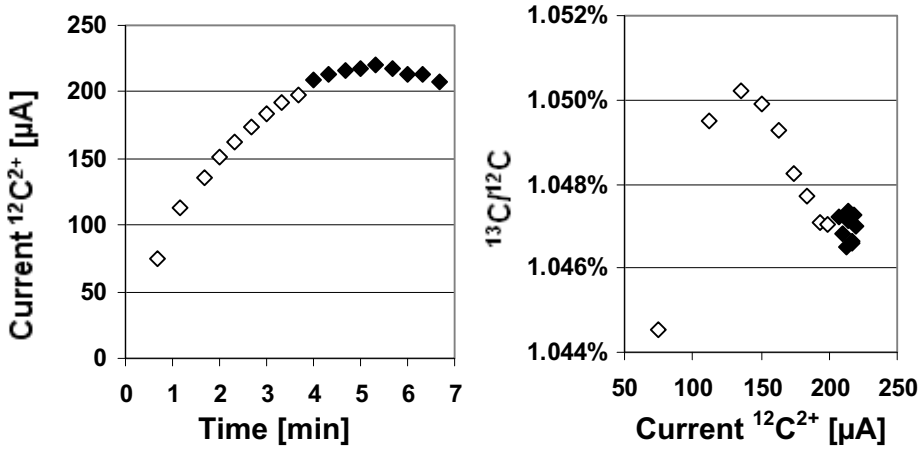

Figure 6 a) Output current as function of measurement time for sample D (left). Empty diamonds represent data included in Figure 5; black diamonds show additional data taken at stable high currents above 200 µA $^{12}C^{2+}$. b) $^{13}C/^{12}C$ ratio versus output current (right).

DISCUSSION AND OUTLOOK

The measurements reveal 2 ranges with different relationships between $^{13}C/^{12}C$ ratio and $^{12}C^{2+}$ current. At high currents, the current dependency of the measured ratios is much smaller. This is most likely related to the fact that the AMS system parameters were fine-tuned while running the source at high output currents. In particular, the einzel lens setting is sensitive to the beam current. With higher current, the beam focus tends to shift further downstream. It is most likely that the observed current dependency below 100 µA would be reduced if the AMS system settings had been readjusted for this current range. For a range of measured output currents spanning over 100 µA, the stability of the $^{13}C/^{12}C$ ratio is ~5‰. For high currents around 200 µA $^{12}C^{2+}$, precision for the $^{14}C/^{12}C$ ratio is entirely dominated by Poisson statistics down to the level of 3‰.

While the dominant bottleneck for particle transmission is the stripper canal, losses due to limited space in the injector magnet chamber may also contribute at currents higher than 200 µA. To cope with this, a high-resolution, large-gap (~62 mm) bouncer injector magnet can replace the present one. With this upgrade, currents ~300 µA ^{12}C may become possible for ^{14}C dating.

CONCLUSIONS

The model SO-110B ion source used in HVE AMS systems supports stable operation at outputs between 100 and 200 µA ^{12}C. The source emittance increases little within this current range, and the optical acceptance of the AMS system is large enough to support the transportation of such high beam currents without significant losses in transmission. The performed measurements suggest the precision for the $^{13}C/^{12}C$ ratio does not degrade when increasing the output and the $^{14}C/^{12}C$ precision is dominated by the Poisson statistics. In addition, the high output current did not affect the measurement background of the system.

REFERENCES

Fallon SJ, Guilderson TP, Brown TA. 2007. CAMS/LLNL ion source efficiency revisited. *Nuclear Instruments and Methods in Physics Research B* 259(1): 106–10.

Freeman SPHT, Cook GT, Dougans AB, Naysmith P, Wilcken KM, Xu S. 2010. Improved SSAMS performance. *Nuclear Instruments and Methods in Physics Research B* 268(7–8):715–7.

Klein M, Mous DJW, Gottdang A. 2004. Fast and accurate sequential injection AMS with gated Faraday cup current measurement. *Radiocarbon* 46(1):77–82.

Klein M, Mous DJW, Gottdang A. 2006. A compact 1MV multi-element AMS system. *Nuclear Instruments and Methods in Physics Research B* 249(1–2): 764–7.

Klein M, Staveren HJ, Mous DJW, Gottdang A. 2007. Performance of the compact HVE 1 MV multi-element AMS system. *Nuclear Instruments and Methods in Physics Research B* 259(1):184–7.

Roberts ML, Burton JR, Elder KL, Longworth BE, McIntyre CP, von Reden KF, Han BX, Rosenheim BE, Jenkins WJ, Galutschek E, McNichol AP. 2010. A high-performance ^{14}C accelerator mass spectrometer. *Radiocarbon* 52(2):228–35.